Study of the shrinkage caused by holographic grating formation in acrylamide based photopolymer film

Mohesh Moothanchery, Izabela Naydenova,* and Vincent Toal

Centre for Industrial & Engineering Optics, School of Physics,
Dublin Institute of Technology Kevin Street, Dublin 8, Ireland
**izabela.naydenova@dit.ie*

Abstract: We study the shrinkage in acrylamide based photopolymer by measuring the Bragg detuning of transmission diffraction gratings recorded at different slant angles and at different intensities for a range of spatial frequencies. Transmission diffraction gratings of spatial frequencies 500, 1000, 1500 and 2000 lines/mm were recorded in an acrylamide based photopolymer film having 60 ± 5 μm thickness. The grating thickness and the final slant angles were obtained from the angular Bragg selectivity curve and hence the shrinkage caused by holographic recording was calculated. The shrinkage of the material was evaluated for three different recording intensities 1, 5 and 10 mW/cm^2 over a range of slant angles, while the total exposure energy was kept constant at 80 mJ/cm^2. From the experimental results it can be seen that the shrinkage of the material is lower for recording with higher intensities and at lower spatial frequencies.

© 2011 Optical Society of America

OCIS codes: (090.0090) Holography; (160.5470) Polymers; (090.7330) Volume gratings; (160.5335) Photosensitive materials; (160.4670) Optical materials.

References and links

1. J. Biles, "Holographic color filters for LCDs," SID Int. Symp. Digest Tech. Papers **25**, 403–406 (1994).
2. A. Pu and D. Psaltis, "High-density recording in photopolymer-based holographic three-dimensional disks," Appl. Opt. **35**(14), 2389–2398 (1996).
3. U.-S. Rhee, H. J. Caulfield, J. Shamir, C. S. Vikram, and M. M. Mirsalehi, "Characteristics of the DuPont photopolymer for angularly multiplexed page-oriented holographic memories," Opt. Eng. **32**(8), 1839–1847 (1993).
4. J. Ludman, H. J. Caulfield, and J. Riccobono, eds., *Holography for the New Millennium* (Springer, 2002), pp. 179–189.
5. G. Ramos, A. Álvarez-Herrero, T. Belenguer, F. del Monte, and D. Levy, "Shrinkage control in a photopolymerizable hybrid solgel material for holographic recording," Appl. Opt. **43**(20), 4018–4024 (2004).
6. S. Martin, C. A. Feely, and V. Toal, "Holographic recording characteristics of an acrylamide-based photopolymer," Appl. Opt. **36**(23), 5757–5768 (1997).
7. I. Naydenova, R. Jallapuram, R. Howard, S. Martin, and V. Toal, "Investigation of the diffusion processes in a self-processing acrylamide-based photopolymer system," Appl. Opt. **43**(14), 2900–2905 (2004).
8. G. Zhao and P. Mouroulis, "Diffusion model of hologram formation in dry photopolymer materials," J. Mod. Opt. **41**(10), 1929–1939 (1994).
9. V. Moreau, Y. Renotte, and Y. Lion, "Characterization of dupont photopolymer: determination of kinetic parameters in a diffusion model," Appl. Opt. **41**(17), 3427–3435 (2002).
10. V. Colvin, R. Larson, A. Harris, and M. Schilling, "Quantitative model of volume hologram formation in photopolymers," J. Appl. Phys. **81**(9), 5913–5923 (1997).
11. J. H. Kwon, H. C. Hwang, and K. C. Woo, "Analysis of temporal behaviour of beams diffracted by volume gratings formed in photopolymers," J. Opt. Soc. Am. B **16**(10), 1651–1657 (1999).
12. S. Piazzolla and B. Jenkins, "First harmonic diffusion model for holographic grating formation in photopolymers," J. Opt. Soc. Am. B **17**(7), 1147–1157 (2000).
13. J. Lawrence, F. O'Neill, and J. Sheridan, "Adjusted intensity nonlocal diffusion model of photopolymer grating formation," J. Opt. Soc. Am. B **19**(4), 621–629 (2002).
14. M. Ortuño, S. Gallego, C. Garcia, C. Neipp, and I. Pascual, "Holographic characteristics of a 1-mm-thick photopolymer to be used in holographic memories," Appl. Opt. **42**(35), 7008–7012 (2003).
15. J. T. Gallo and C. M. Verber, "Model for the effects of material shrinkage on volume holograms," Appl. Opt. **33**(29), 6797–6804 (1994).

#144225 - $15.00 USD Received 16 Mar 2011; revised 18 Apr 2011; accepted 19 Apr 2011; published 27 Jun 2011

16. C. Neipp, A. Beléndez, S. Gallego, M. Ortuño, I. Pascual, and J. T. Sheridan, "Angular responses of the first and second diffracted orders in transmission diffraction grating recorded on photopolymer material," Opt. Express **11**(16), 1835–1843 (2003).
17. H. Sherif, I. Naydenova, S. Martin, C. McGinn, and V. Toal, "Characterization of an acrylamide-based photopolymer for data storage utilizing holographic angular multiplexing," J. Opt. A, Pure Appl. Opt. **7**(5), 255–260 (2005).
18. C. Zhao, J. Liu, Z. Fu, and R. T. Chen, "Shrinkage correction of volume phase holograms for optical interconnects," Proc. SPIE **3005**, 224–229 (1997).
19. I. Naydenova, H. Sherif, S. Mintova, S. Martin, and V. Toal, "Holographic recording in nanoparticle doped photopolymer," Proc. SPIE **6252**, 625206 (2006).
20. I. Naydenova, E. Leite, T. Babeva, N. Pandey, T. Baron, T. Yovcheva, S. Sainov, S. Martin, S. Mintova, and V. Toal, "Optical properties of photopolymerisable nanocomposites containing nanosized molecular sieves," J. Opt. **13**(4), 044019 (2011).
21. E. Mihaylova and V. Toal, "Simple versatile shearing interferometer suitable for measurements on a microscopic scale," Opt. Lasers Eng. **47**(2), 271–273 (2009).

1. Introduction

Photopolymers have been investigated for many years for holographic applications including LCD displays [1] data storage [2,3] optical elements [4] etc. because of their easy processing, high light sensitivity, relatively high refractive index contrast and low cost. One of the main challenges in the implementation of photopolymers in holographic applications is the rotation of Bragg angle due to change in volume [5]. Such changes can be observed in transmission and reflection holographic gratings. The material under study here is an acrylamide based photopolymer developed at the Centre for Industrial and Engineering Optics [6,7]. Holographic characteristics such as diffraction efficiency and angular selectivity profile were measured. In this paper we consider the parameters which may influence the shrinkage such as recording intensity, spatial frequencies and the thickness of the photopolymer layers. The mechanism of hologram formation in photopolymer is a complicated process which involves polymerization and diffusion of photopolymer components and has been explained in detail [8–14].

Hologram formation in photopolymers is a three-step process. First the photopolymer is exposed to the interference pattern to be recorded. This initial exposure polymerizes some of the monomers. The monomer concentration gradients due to spatial variation in the amount of polymerization which give rise to the diffusion of the relatively small monomer molecules from regions of higher concentration to regions of lower concentration. It is well known that the diffusion of monomer plays a vital role during holographic recording [8]. In addition short chain polymer molecules formed in illuminated regions can diffuse into dark fringe regions [7]. It is common observation that during the polymerization process the material shrinks and its refractive index increases. We have studied how the recording intensity, layer thickness and spatial frequency of recording influence the dimensional change (usually shrinkage) in the photopolymer layer.

We are concerned primarily with the thickness change in the direction perpendicular to the surface of the substrate. Three different photopolymerization processes influence the thickness variation of the photopolymer films. They are (1) polymerization modulation due to the spatial modulation of intensity in the interference pattern of the two recording beams; (2) bulk polymerization due to the spatial average of the intensity of the two beams; and (3) UV curing and baking processes after recording [15].

Up to now there has not been a detailed experimental study of shrinkage in acrylamide based photopolymers which takes into account simultaneously the layer thickness and recording parameters such as light intensity and spatial frequency. Such studies provide in depth information about the physical process influencing the photoinduced dimensional changes of the layers [16–19]. The angular shifts of the positions of Bragg peaks for slanted holographic gratings were determined after recording. We obtained the Bragg curves of the slanted holographic gratings after recording and analysing the angular Bragg selectivity curves. The curves were fitted using Kogelnik's coupled wave theory as explained in [19]. One can write the expression for the fractional change Δd in grating thickness d knowing the

#144225 - $15.00 USD Received 16 Mar 2011; revised 18 Apr 2011; accepted 19 Apr 2011; published 27 Jun 2011
(C) 2011 OSA

initial and the final slant angles as explained in [15]. Hence the shrinkage can be calculated using

$$\frac{\Delta d}{d} = \frac{\tan\varphi_1}{\tan\varphi_0} - 1 \tag{1}$$

where ϕ_0 and ϕ_1 are respectively the slant angles of the grating at the start and end of the recording process.

2. Experimental procedure

2.1 Sample preparation

The composition of the photopolymer solution used to prepare the layers for holographic recording is as shown in Table 1.

Table 1. Photopolymer Composition

Acrylamide	0.6g
Methylenebisacrylamide	0.2g
Polyvinyl alcohol (10% wt./v stock)	17.5ml
Triethanolamine	2ml
Erythrosine B dye (0.11%wt./wt.)	4ml

The photopolymer layer was prepared as described in [6]. Briefly, 0.6g of acrylamide monomer was added to 17.5 ml stock solution of polyvinyl alcohol (10% wt/v). Then 2ml of triethanolamine was added. To this solution 0.2 g of *N*, *N*_-Methylenebisacrylamide and finally 4ml of Erythrosin B dye was added (0.11% wt/wt stock solution). Of this solution, 1.2 ml was spread on a 25 mm x 120 mm glass plate. The samples were dried for 24 h. Sample thickness after drying was 60 ± 5 μm.

2.2 Holographic recording

The optical setup for recording holographic gratings is shown in Fig. 1 in which the 532 nm beam from a frequency doubled Nd-YVO4 laser was spatially filtered, expanded and collimated to around 1cm cross sectional diameter and split into two beams using a beamsplitter. The beams were made to overlap completely at the sample of photopolymer at equal and opposite angles of incidence to ensure that the beam ratio was constant across the illuminated area and that the grating was initially unslanted. The angles between the two recording beams outside the layers were 15.29°, 30.85°, 47.03° and 64.28° so that the spatial frequencies were approximately 500, 1000, 1500 and 2000 lines/mm respectively. The photosensitive layer was mounted on a high-precision computer-controlled rotational stage (Newport M-URM100ACC). Gratings were recorded using intensities of 1, 5 and 10 mW/cm^2 and exposure times 80, 16 and 8s.

The angular selectivity curves for gratings recorded in layers of 3 different thicknesses 30, 60 and 120 μm with recording intensity 10 mW/cm^2 were also measured. The diffraction efficiencies of the gratings were monitored in real time using a He-Ne beam which was diffracted by the recorded grating but not absorbed by the photopolymer layer.

#144225 - $15.00 USD Received 16 Mar 2011; revised 18 Apr 2011; accepted 19 Apr 2011; published 27 Jun 2011
(C) 2011 OSA

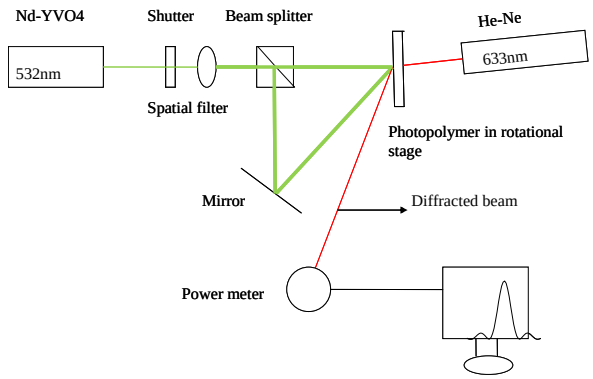

Fig. 1. Optical set-up for recording transmission phase holographic gratings.

The intensity of the He-Ne laser incident on the grating and the diffracted intensity were both measured using a power meter (Newport Optical Power Meter (Model 1830-C). It was necessary to ensure that the He–Ne laser was incident at the Bragg angle for 633-nm light. We first recorded unslanted grating, for which no shift of the Bragg peak was expected. It was observed that there was a small deviation (± 0.017°) in the position of maximum diffraction intensity outside the photopolymer layer from the expected angular position (0°). In our further experiments a correction for the zero position due to these imperfections in the initial alignment of the unslanted grating was made.

After acquiring the angular selectivity profiles for unslanted gratings the profiles of gratings recorded with slant angles of + 5°, + 10°, –5° and –10° were measured. Angular selectivity curves inside the layer were fitted to the data with Microcal Origin software applying Kogelnik's coupled wave theory, from which we obtained the positions of the Bragg peaks (ϕ_0 and ϕ_1) and the thicknesses of the gratings *(d)*. The angular selectivity curves inside the layer were plotted after taking into account the refractive index of the layer (1.499 ± 0.002) which was previously characterized and reported in [20]. The angular detuning caused by shrinkage was corrected for any initial Bragg detuning with respect to the incident angle of the He-Ne probe beam. All measurements were carried out at constant humidity and temperature in order to avoid any influence of the environment on the shrinkage/swelling of the photopolymer layer.

#144225 - $15.00 USD Received 16 Mar 2011; revised 18 Apr 2011; accepted 19 Apr 2011; published 27 Jun 2011
(C) 2011 OSA

3. Results and discussion

3.1 Intensity dependence

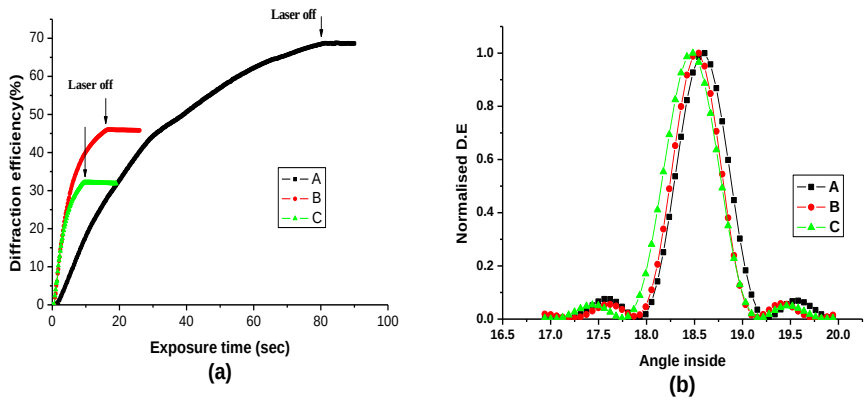

Fig. 2. Diffraction efficiency growth (a) and angular selectivity curves (b) for gratings recorded at A(-■-) 1mW/cm^2, 80sec; B (-●-) 5mW/cm^2, 16sec, C (-▲-) 10mW/cm^2, 8sec. The corresponding peak positions in (b) are A (-■-)18.525°; B (-●-)18.483° ; C (-▲-) 18.468°.

Figure 2(a) shows the growth curves of 10° slanted gratings for three different intensities. Figure 2(b) shows the angular selectivity curves of the gratings of 1000 lines/mm recorded at the same slant angle. From the graph one can see a shift in the peak position of the curve due to shrinkage and the shift is greater for gratings recorded with lower intensities and longer exposure times, i.e. 1 mW/cm^2 and 80s. The same intensity dependence was observed for all other slant angles (+ 5°, –5°, –10°). The change in refractive index of the photopolymer was taken into account when calculating the shrinkage

3.2 Spatial frequency dependence

We can also derive the dependence of shrinkage on spatial frequency from Fig. 3 which shows growth curves of 10° slanted gratings for four different spatial frequencies, Fig. 3(a). Figure 3(b) shows the angular selectivity curves of these gratings. These angular selectivity curves obtained after recording were fitted using Origin giving the final peak position. The initial peak position was obtained from the spatial frequency and hence the shift in Bragg peak can be determined. The Bragg curves show larger shifts of peak position for recordings at higher spatial frequencies of 2000 lines/mm and lower shift for spatial frequency of 500 lines/mm. Figure 4 shows the corresponding shifts of Bragg peaks inside the layers at different spatial frequencies (a) 500 lines/mm, (b) 1000 lines/mm, (c) 1500 lines/mm, (d) 2000 lines/mm for three different intensities of recording.

#144225 - $15.00 USD Received 16 Mar 2011; revised 18 Apr 2011; accepted 19 Apr 2011; published 27 Jun 2011
(C) 2011 OSA

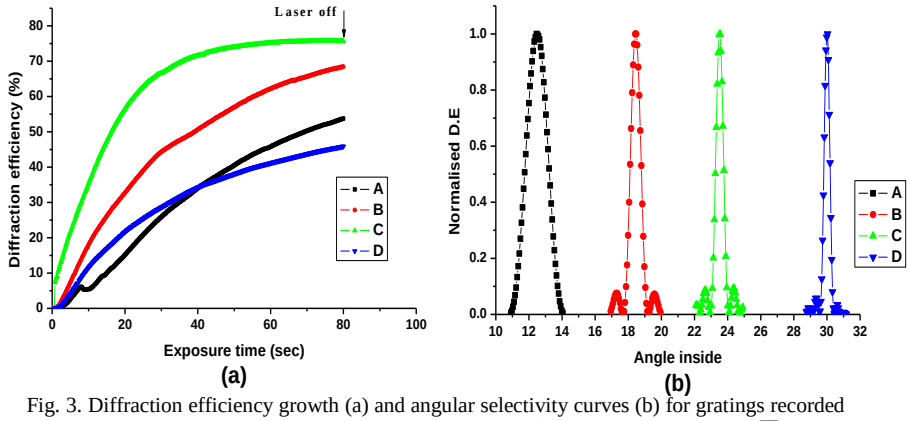

Fig. 3. Diffraction efficiency growth (a) and angular selectivity curves (b) for gratings recorded at A (-■-) 500 lines/mm; B (-●-) 1000 lines/mm, C (-▲-) 1500 lines/mm, D (-▼-) 2000 lines/mm. The corresponding shift in Bragg peak in (b) is A (-■-) 0.08°; B (-●-) 0.12°; C (-▲-) 0.15°; D (-▼-) 0.3°.

One can notice in Fig. 4 that there is a pronounced dependence of the shift in the Bragg angular selectivity curve at lower spatial frequency of recording and almost no dependence at high spatial frequency of recording. The difference between the high and low spatial frequencies of recording is the fringe spacing and thus the distance travelled by the monomer molecules due to the concentration gradient driven diffusion from the dark to the bright fringes, where they are polymerized.

#144225 - $15.00 USD Received 16 Mar 2011; revised 18 Apr 2011; accepted 19 Apr 2011; published 27 Jun 2011
(C) 2011 OSA

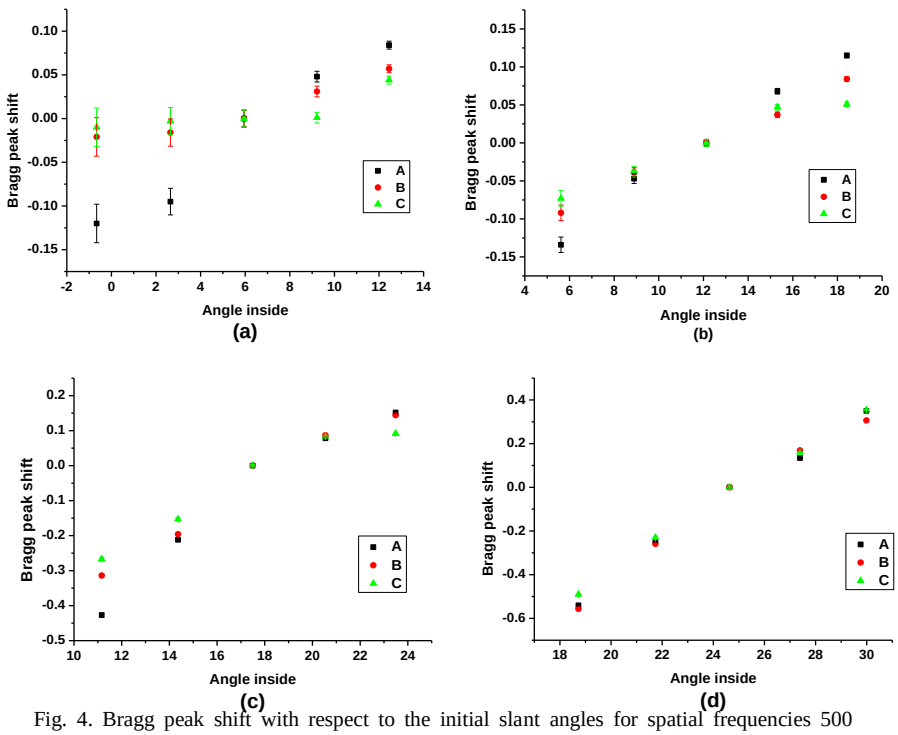

Fig. 4. Bragg peak shift with respect to the initial slant angles for spatial frequencies 500 lines/mm (a) 1000 lines/mm (b), 1500 lines/mm(c) and 2000 lines/mm(d) for gratings recorded at A (■) –1 mW/cm^2; B (●)- 5 mW/cm^2, C (▲)- 10 mW/cm^2.

One can determine the shrinkage caused due to holographic recording using Eq. (1). Figure 5 shows the tangent of final slant angle versus tangent of initial slant angle for gratings recorded at 10 mW/cm^2 at 1000 lines/mm and the slope gives the percentage shrinkage of the material. The percentage shrinkage evaluated from the curve is 1.08%. Similarly the shrinkage can be calculated for different recording intensities and spatial frequencies.

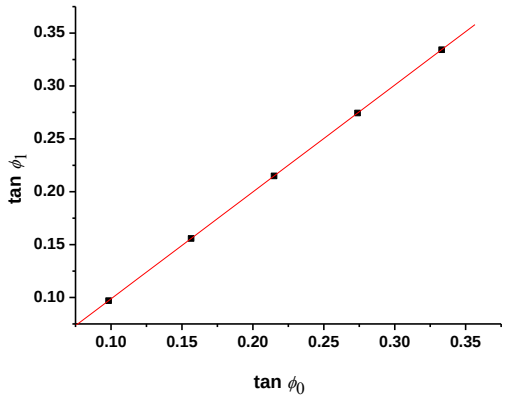

Fig. 5. Dependence of the new slant angle on the initial slant angle for recording intensity 10mW/cm^2 . at 1000 lines/mm, shrinkage-1.08%.

#144225 - $15.00 USD Received 16 Mar 2011; revised 18 Apr 2011; accepted 19 Apr 2011; published 27 Jun 2011
(C) 2011 OSA

We summarise the dependence of shrinkage on recording intensity and spatial frequency in Fig. 6, which shows plots of shrinkage versus spatial frequency for three different recording intensities. We can correlate the increased shrinkage at lower intensities of exposure and higher spatial frequencies with the fact that at lower illumination intensity the polymer molecules formed are likely to be larger. The reason for this is that the rate at which the free radicals are generated is smaller and thus the volume concentration of free radicals is lower. This leads to a lower rate of termination and the ultimate result is the creation of longer polymer chains each comprising a larger number of monomer molecules. It is known that the polymerised material has higher density due to the morphology of the polymer material made of entangled polymer molecules.

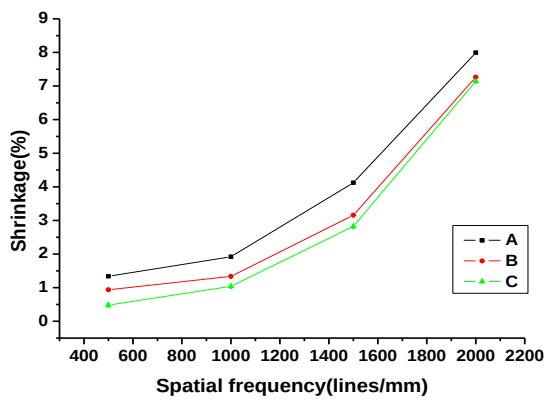

Fig. 6. Dependence of shrinkage on spatial frequency for recording intensities A (-■-) 1 mW/cm^2, B (-●-) 5mW/cm^2, C (-▲-) 10 mW/cm^2 for 60 ± 5 μm layers.

For a greater extent of polymerization the final density and thus the total dimensional change of the layer is expected to be greater. The experimental results imply that careful consideration should be given to the recording conditions if shrinkage is to be avoided. Higher intensities and lower spatial frequencies are recommended but the maximum achievable diffraction efficiency is lower in these cases (Figs. 2(a) and 3(a)). The shrinkage is expected to depend on the thickness of the layers because the rate of polymerisation occurring in thicker layers is different in comparison to the rate in thinner layers. The next set of experiments was carried out in layers of three different thicknesses 30, 60 and 120μm.

3.3 Thickness dependence

Figure 7(a) shows the growth curves of 5° slanted gratings recorded with three different thicknesses at 1000 lines/mm. Figure 7(b) shows the corresponding angular selectivity curves. One can notice a shift in the peak position of the curve due to shrinkage and the shift is greater for gratings recorded in thinner layers. Similar thickness dependence of the shift was observed for all other slant angles (+ 10°, −5°,-10°).The same refractive index modulation is obtained for layers of thickness 30, 60 and 120μm, Fig. 8(a), suggesting the same extent of monomer molecule conversion per unit volume-thus the same absolute shrinkage. Figure 8(b) shows the percentage shrinkage versus thickness. Knowing the percentage shrinkage and the thickness of layers the absolute shrinkages were calculated for the three sets of layers were respectively 0.474 ± 0.003, 0.648 ± 0.003 and 0.696 ± 0.004μm.

#144225 - $15.00 USD Received 16 Mar 2011; revised 18 Apr 2011; accepted 19 Apr 2011; published 27 Jun 2011
(C) 2011 OSA

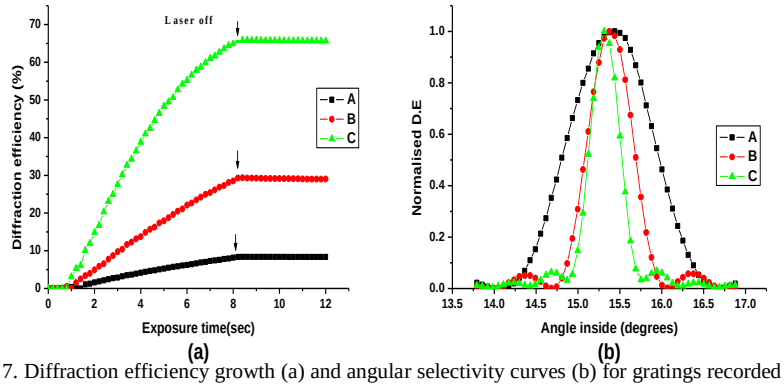

Fig. 7. Diffraction efficiency growth (a) and angular selectivity curves (b) for gratings recorded in layers of thickness A (-■-) 30 μm; B (-●-) 60 μm, C (-▲-) 120 μm. The corresponding position of Bragg peak in (b) are A (-■-) 15.441°, B (-●-) 15.375°,C (-▲-) 15.31°.

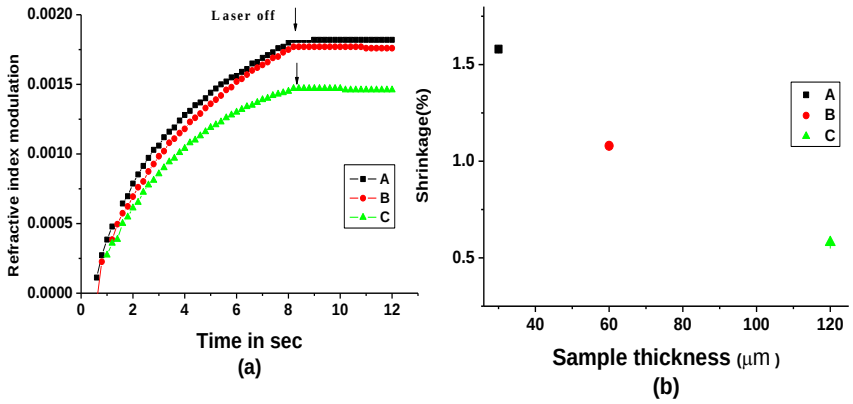

Fig. 8. Dependence of refractive index modulation with exposure time (a) and percentage shrinkage on sample thickness (b) for thickness A (■) –30μm, B (●) –60μm, C (▲)-120μm.

In order to confirm the larger shrinkage at high spatial frequency of recording, gratings were recorded at 2000 lines/mm in 50 μm and 105 μm thick layers exposed to 5 mW/cm^2 for 16 sec. The dimensional changes of the layers after recording of the holographic gratings were measured using a white light interferometric profiler [21]. It was calculated that the shrinkage of these layers respectively was 8.2% (4.1 μm absolute shrinkage) and 3.14% (3.3 μm absolute shrinkage). These values for the shrinkage are consistent with the result obtained in Fig. 6, where for the same recording conditions (curve B) in 60μm thick layers the shrinkage was evaluated to be 7.27% (4.4μm absolute shrinkage). One possible explanation for the large values of the observed shrinkage at high spatial frequency is the larger number of monomer molecules converted into polymer molecules, causing larger density change. At high spatial frequency the distance travelled by the monomer molecules from the dark to the bright fringes is smaller. During a given exposure time a larger number of monomer molecules will manage to reach the bright fringes at higher spatial frequency of recording than the number of monomers transported at lower spatial frequency of recording. Thus a larger number of monomer will be polymerised at higher spatial frequency of recording and larger dimensional change (shrinkage) is expected.

#144225 - $15.00 USD Received 16 Mar 2011; revised 18 Apr 2011; accepted 19 Apr 2011; published 27 Jun 2011
(C) 2011 OSA

4. Conclusions

Transmission diffraction gratings of different spatial frequencies were recorded in an acrylamide based photopolymer film having 60 ± 5 μm thickness at constant exposure and different intensities and exposure times. We have obtained the angular Bragg selectivity curves and Kogelnik's coupled wave theory was used to fit them. We have obtained grating thickness and final slant angles from the Bragg curve and hence calculated the shrinkage. Higher shrinkage was measured for recording with lower intensity and longer time of exposure and also at higher spatial frequencies. We also determined the percentage shrinkage at three different thicknesses and the percentage shrinkage is lower for recording with thicker layers.

The next step is the modification of the photopolymer material in order to decrease the shrinkage due to photopolymerisation. We are studying the effect of incorporating different nanoparticles in the material. The results will be presented elsewhere.

Acknowledgment

This work was supported by a scholarship provided by the Technological Sector Research: Strand I—Post-Graduate R&D Skills Programme. The authors would like to acknowledge the School of Physics and FOCAS, DIT for technical support. The financial support of the SARA Programme, DIT is also acknowledged.